

# Higher modes of vibration increase mass sensitivity in nanomechanical microcantilevers

Murali Krishna Ghatkesar<sup>1,3</sup>, Viola Barwich<sup>1,3</sup>, Thomas Braun<sup>1,3</sup>,  
Jean-Pierre Ramseyer<sup>1</sup>, Christoph Gerber<sup>1</sup>, Martin Hegner<sup>1</sup>,  
Hans Peter Lang<sup>1,2</sup>, Ute Drechsler<sup>2</sup> and Michel Despont<sup>2</sup>

<sup>1</sup> National Center of Competence for Research in Nanoscience, Institute of Physics,  
University of Basel, 4056 Basel, Switzerland

<sup>2</sup> IBM Research GmbH, Zurich Research Laboratory, 8803 Rüschlikon, Switzerland

E-mail: [hans-peter.lang@unibas.ch](mailto:hans-peter.lang@unibas.ch)

Received 17 July 2007, in final form 14 September 2007

Published 9 October 2007

Online at [stacks.iop.org/Nano/18/445502](http://stacks.iop.org/Nano/18/445502)

## Abstract

We evaluated the potential and limitations of resonating nanomechanical microcantilevers for the detection of mass adsorption. As a test system we used mass addition of gold layers of varying thickness. Our main findings are: (1) A linear increase in mass sensitivity with the square of the mode number—a sensitivity increase of two orders of magnitude is obtained from mode 1 to mode 7 with a minimum sensitivity of  $8.6 \text{ ag Hz}^{-1} \mu\text{m}^{-2}$  and mass resolution of 0.43 pg at mode 7 for a  $1 \mu\text{m}$  thick cantilever. (2) The quality factor increases with the mode number, thus helping to achieve a higher sensitivity. (3) The effective spring constant of the cantilever remains constant for deposition of gold layers up to at least 4% of the cantilever thickness.

(Some figures in this article are in colour only in the electronic version)

## 1. Introduction

Microfabricated mechanical structures like cantilevers and beams operated at their resonance frequency are used as extremely sensitive mass detectors. Mass adsorption on these resonators shifts their resonance frequency. The aim is to reach maximum sensitivity (maximum frequency shift for a given mass change) and resolution (minimum detectable mass). In this pursuit, zeptogram ( $10^{-21}$  g) sensitivity obtained in a vacuum has been recently reported [1]. A general approach to gain higher sensitivity is to reduce the inertial mass of the resonating sensor itself. Increase in mass sensitivity from pg to fg was achieved by reducing the volume of the device by  $\sim 1000$  times [2]. Different sensor geometries and various materials are also used to measure small masses [3–5].

Assuming that the spring constant of a microcantilever remains unchanged, the mass sensitivity is given as

$$S = \frac{\Delta f}{\Delta m} = \frac{f_{R,n}}{2m_c}, \quad (1)$$

where  $\Delta f$  is the frequency shift for a mass addition of  $\Delta m$  and  $f_{R,n}$  is the resonance frequency at a mode number  $n$  for a cantilever of mass  $m_c$ . The frequency shift obtained for a unit mass adsorbed on a given cantilever is directly proportional to the resonance frequency at mode number  $n$ . Hence, for the same cantilever dimensions, the sensitivity can be increased by operating the cantilever at higher modes of vibration.

For biological and chemical applications of these sensors a distributed mass load spanning the entire cantilever surface is preferred instead of a mass load at a selected area [6–11]. This prevents the need for selective activation of the surface and avoids unspecific binding.

To mimic such situations, we used cantilevers with gold layer deposits of different thicknesses on the entire upper surface of the cantilever. Moreover, the cantilever thickness was also varied between 1 and 7  $\mu\text{m}$ . The frequency response of the cantilevers was measured and evaluated at

<sup>3</sup> These authors made an equal contribution to this work.

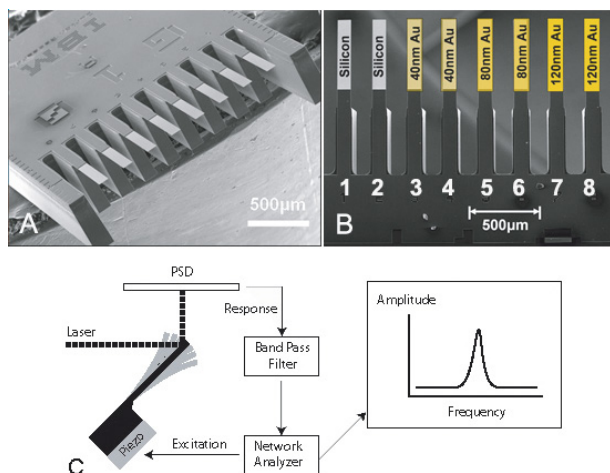


**Figure 1.** (A) An array of eight cantilevers having the same dimensions of length, width and thickness. (B) Different thicknesses of gold coating on the cantilever array. Sets of two cantilevers each were chosen for the deposition of gold layers 40, 80 and 120 nm thick. This was achieved using a shadow mask, exposing two cantilevers for every 40 nm of successive gold depositions. Two cantilevers were left as bare silicon for reference. (C) Experimental setup for the measurement. A linear frequency sweep with a sinusoidal signal from a network analyzer excites the piezo beneath the cantilever. Cantilever vibrations were detected by a laser beam deflection technique. The output signal detected was limited from 500 Hz to 1 MHz by a band pass filter. Input and output signals were compared in the network analyzer to give a resonance spectrum.

various flexural modes of vibration before and after gold layer deposition.

## 2. Experimental details

Three different types of cantilever array with eight identical Si cantilevers each 500  $\mu\text{m}$  long and 100  $\mu\text{m}$  wide, but different thicknesses of 7  $\mu\text{m}$ , 4  $\mu\text{m}$  and 1  $\mu\text{m}$ , respectively, were used. The cantilever arrays of thickness 7 and 4  $\mu\text{m}$  were wet etched out of Si wafer while the 1  $\mu\text{m}$  thick cantilevers were dry etched out of silicon on insulator (SOI) wafer. They were microfabricated by the Micro and Nanomechanics Group, IBM Zurich Research Laboratory in Rueschlikon, Switzerland. A scanning electron microscope (SEM) image of an individual array chip is shown in figure 1(A).

### 2.1. Preparation of the cantilevers

Layers of different thickness of gold were deposited on the upper side of the cantilevers with an initial titanium (99.99%, Johnson Matthey, London, UK) adhesion layer of 2 nm between Si and gold (99.999%, Goodfellow, Bad Nauheim, Germany). All depositions were done in a Balzers MED 010 thermal evaporator operated at a base pressure below  $10^{-5}$  mbar with evaporation rates of  $0.16 \text{ nm s}^{-1}$ . Three layers of 40 nm thick gold were deposited successively. A shadow mask was used to physically cover cantilevers numbered (see figure 1(B)) one to six for the first deposition, one to four for the second deposition and finally one and two for the third deposition. After three successive depositions, cantilevers numbered 1 and 2 were obtained with no gold, 3 and 4

with 40 nm, 5 and 6 with 80 nm and 7 and 8 with 120 nm thick gold layers, respectively. The density values used for silicon, titanium and gold were  $\rho_{\text{Si}} = 2330 \text{ kg m}^{-3}$ ,  $\rho_{\text{Ti}} = 4990 \text{ kg m}^{-3}$  and  $\rho_{\text{Au}} = 19320 \text{ kg m}^{-3}$ , respectively. The corresponding elastic moduli values used were  $E_{\text{Si}} = 169 \text{ GPa}$ ,  $E_{\text{Ti}} = 110 \text{ GPa}$  and  $E_{\text{Au}} = 69 \text{ GPa}$ , respectively.

### 2.2. Setup

Ambient thermal excitation of the cantilevers was not sufficient to detect the various vibrating modes. This is due to the fact that some of the cantilevers chosen has a high spring constant value. Furthermore, the value of the spring constant increases with the mode number [12]. For these reasons, the cantilevers were driven externally by a piezo. The drive amplitude was kept low to avoid invoking nonlinearities in the cantilever vibrations and to satisfy the simple harmonic oscillator (SHO) condition. The aspect ratio of all the cantilevers was  $L/b = 5$  and the amplitude of vibration is low compared to any dimension of the cantilever. The experimental setup used for the measurement is shown in figure 1(C). The cantilever array was mounted on a piezo element PZT-5A purchased from Staveley Sensors (East Hartford, CT, USA). By placing the piezo beneath the cantilever chip body in direct contact, the excitation energy was efficiently transferred to the cantilevers. For a linear frequency sweep with a sinusoidal signal from the network analyzer (Hewlett Packard, 4589A, USA), cantilevers were excited at various vibrating modes. A laser beam deflection technique was used to detect frequencies of the cantilever vibrations [13]. Time multiplexed laser light emitted sequentially from eight vertical cavity surface emitting lasers (VCSEL; wavelength 760 nm, Avalon Photonics, Zurich, Switzerland) deflected from the apex of the cantilever to a 1D position-sensitive detector (PSD; Sitek, Partille, Sweden) [14] was used. The pitch of the VCSELs matches that of the cantilevers. The output signal current of the PSD was converted into voltage and band pass filtered (BPF) form in a bandwidth range of 500 Hz to 1 MHz. The network analyzer converted the time domain signals into a frequency spectrum with peaks corresponding to the different resonating flexural modes of the cantilever.

The resonance frequencies of all cantilevers at various modes were recorded before and after gold coating. All measurements were performed in ambient air. Initially a complete spectrum with resonance peaks corresponding to all the modes was recorded. Then each mode was individually recorded to determine the corresponding value of the resonance frequency peak with higher resolution.

## 3. Theory

### 3.1. Resonance frequency

The resonance frequency of a vibrating cantilever at an arbitrary mode number  $n$  in a vacuum is given as

$$f_{R,n}^{\text{theo}} = \frac{\alpha_n^2}{2\pi} \sqrt{\frac{EI}{m_c l^3}}, \quad (2)$$

where  $E$  is the elastic modulus of the material,  $I$  is the moment of inertia of the cantilever,  $l$  is its length,  $b$  its width,  $h$  its

thickness,  $m_c$  its mass and constants  $\alpha_1 = 1.875$ ,  $\alpha_2 = 4.694$ ,  $\alpha_3 = 7.854$ ,  $\alpha_4 = 11.0$ ,  $\alpha_{5\dots n} = \pi(n - 0.5)$  [15]. The value  $n = 1$  refers to the fundamental mode or mode 1. In practice, cantilevers are never ideal, they can have internal defects or imperfections from the etching process. These features can contribute to deviation of resonance frequencies from the theoretical predicted values. To account for such deviations, we introduce a correction factor  $C$  to equation (2) as follows:

$$f_{R,n} = C \frac{\alpha_n^2}{2\pi} \sqrt{\frac{EI}{m_c l^3}}, \quad (3)$$

where

$$C = \frac{f_{R,n} \alpha_1^2}{f_{R,1} \alpha_n^2} \quad (4)$$

with  $f_{R,n}$  and  $f_{R,1}$  being the resonance frequencies measured experimentally at mode  $n$  and mode 1.  $C = 1$  for an ideal cantilever for all modes.

The resonance frequency and quality factor for each mode are obtained by fitting the corresponding frequency spectrum to a SHO function as shown in equation (5) with fitting parameters being  $A_0$ ,  $f_{R,n}$  and  $Q$  [16]:

$$A(f) \cong \frac{A_0 f_{R,n}^2}{\sqrt{(f^2 - f_{R,n}^2)^2 + \frac{f_{R,n}^2}{Q^2}}}, \quad (5)$$

where  $A_0$  is the zero-frequency amplitude of the response and  $Q$  is the quality factor of the mode. Note that the SHO condition is satisfied only for  $Q \geq 1$ ,  $L/b \geq 4$  and without invoking nonlinearities in vibration [16].

### 3.2. Calculation of mass

During Au layer deposition on the microcantilevers, a quartz crystal microbalance placed adjacent to arrays determines the thickness of the layer deposited. Considering the Ti adhesion layer deposited between the Si cantilever and the Au layer, the mass calculated on a single cantilever is

$$\Delta m_q = \rho_{Ti} l b h_{Ti} + \rho_{Au} l b h_{Au} \quad (6)$$

where  $h_{Ti}$  and  $h_{Au}$  are the thickness of Ti and Au, respectively. This mass will be compared with the mass obtained by change in the resonance frequency of the cantilever.

The calculation of mass from the resonance frequency shift of the cantilever vibrations is carried out in two ways, termed the 'mass only effect' and the 'mass and spring constant effect'. In the 'mass only effect', the frequency shift obtained is considered to be due only to the change in mass on the cantilever, while in the 'mass and spring constant effect', the spring constant values of Ti and Au layers are also considered along with their respective mass. Cantilevers were considered as composite structures and from equation (3) we derive

$$\Delta m_m = C^2 \frac{\alpha_n^4}{4\pi^2 l^3} EI \left( \frac{1}{f_{R,n}^2} - \frac{1}{f_{R,n}^{\prime 2}} \right), \quad (7)$$

where  $\Delta m_m$  is the mass according to the 'mass only effect' and  $f_{R,n}^{\prime}$  is the frequency after the Au layer deposition:

$$\Delta m_{mk} = C^2 \frac{\alpha_n^4}{4\pi^2 l^3} \left( \frac{\sum_{i=0}^3 E_i I_i}{f_{R,n}^2} - \frac{EI}{f_{R,n}^{\prime 2}} \right) \quad (8)$$

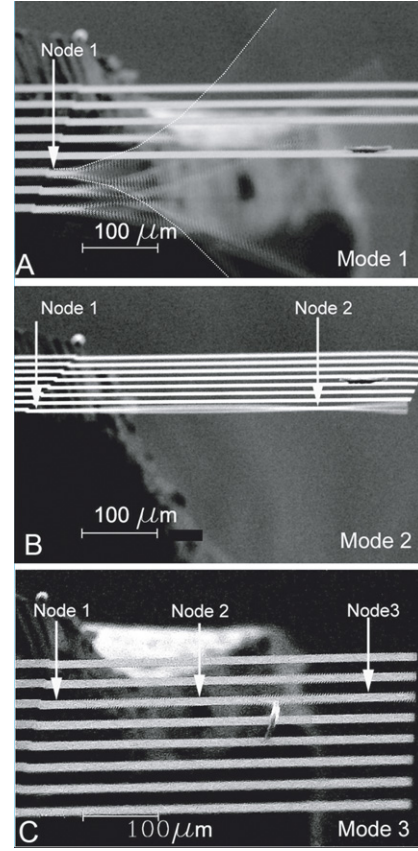


**Figure 2.** SEM images of cantilever vibrations for the first three modes. The number of nodes defines the mode number: (A) mode 1, (B) mode 2, (C) mode 3. The antinodes in mode 3, which are very low in the vertical vibration amplitude of the cantilever, are observed to be 'hazy' compared to well focussed nodes on the indicated cantilever.

where  $\Delta m_{mk}$  is the mass due to the 'mass and spring constant' effect and the sum of 3 corresponds to three different materials: Si, Ti and Au [17].

## 4. Results

### 4.1. Visualization of resonance modes

Various modes of vibration were visualized using a scanning electron microscope (SEM). Figure 2 shows images of the first three modes obtained for a 1  $\mu\text{m}$  thick cantilever. Nodes and antinodes were clearly visible for mode 1 and mode 2, but they are barely visible for mode 3. Visualizing them after mode 3 was impossible using the SEM as the vertical amplitude of the vibrating cantilever was beyond its resolution. The observation also indicates that not all the cantilevers have the same resonance frequency. The difference was more prominent at higher modes. The observed high amplitudes of the vibrating cantilevers were due to the high excitation voltage used just for visualizing the modes. Actual experiments for mass measurements were done at low amplitudes (<5 nm) of vibration, within limits of the SHO condition for a vibrating cantilever. For 4 and 7  $\mu\text{m}$  cantilevers only the first mode was observed (pictures not shown).

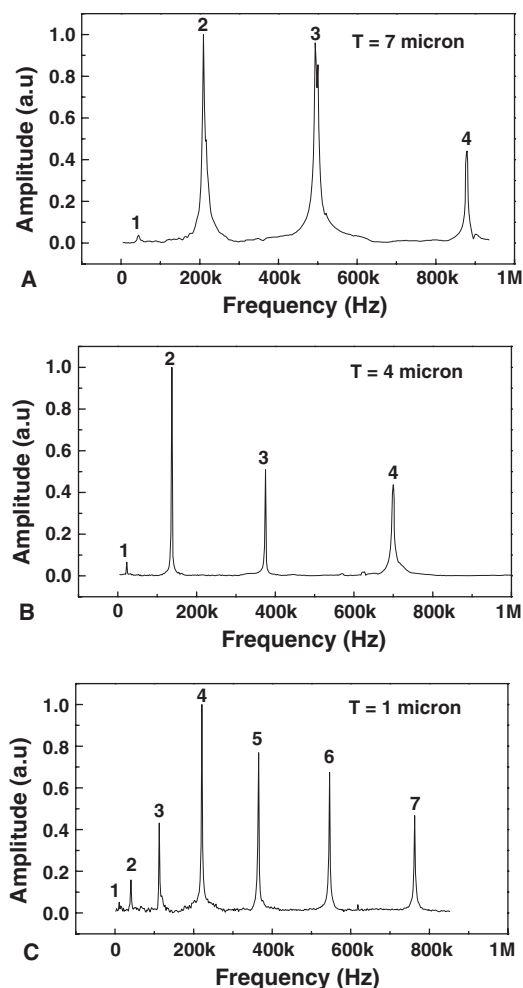


**Figure 3.** Complete spectra of resonance frequencies up to 1 MHz. All cantilevers are 500  $\mu\text{m}$  long and 100  $\mu\text{m}$  wide: (A) 7  $\mu\text{m}$  thick, (B) 4  $\mu\text{m}$  thick and (C) 1  $\mu\text{m}$  thick. More modes were visible for thinner cantilevers. The spacing between adjacent modes increased with the mode number.

#### 4.2. Frequency spectra

The frequency spectra up to 1 MHz obtained for all the cantilevers are shown in the figure 3. Only four modes were observed for 7 and 4  $\mu\text{m}$  thick cantilevers, while the 1  $\mu\text{m}$  thick cantilever exhibited seven modes. As the thickness of the cantilever decreased, higher modes shifted to lower frequency values. Hence, more modes were visible in the same frequency range. The frequencies and the corresponding quality factors of all the cantilevers are given in table 1. The values shown correspond to a single cantilever and the standard deviation of frequency among eight cantilevers in an array was  $\leq 0.1\%$ . The quality factor increased with mode number. The frequency spacing between adjacent modes also increased with mode number. The spring constants calculated from the respective fundamental frequencies are  $k_{7\mu\text{m}} = 9.6 \text{ N m}^{-1}$ ,  $k_{4\mu\text{m}} = 2.3 \text{ N m}^{-1}$  and  $k_{1\mu\text{m}} = 0.05 \text{ N m}^{-1}$ , respectively.

#### 4.3. Calibration

For a cantilever vibrating in a medium the resonance frequencies shift to lower values compared to their corresponding val-

**Table 1.** Resonance frequency and corresponding quality factor values of various modes of 7, 4 and 1  $\mu\text{m}$  thick bare silicon cantilevers measured up to 1 MHz in ambient air. The standard deviation among eight cantilevers in an array is  $\leq 0.1\%$ . In the frequency range up to 1 MHz, the cantilever with a thickness of 1  $\mu\text{m}$  has seven modes compared to only four modes for the 4 and 7  $\mu\text{m}$  thick cantilevers. The quality factor increased with the mode number and the frequency spacing between adjacent modes also increased.

n	Mode					
	7 $\mu\text{m}$		4 $\mu\text{m}$		1 $\mu\text{m}$	
	$f_{R,n}$	Q	$f_{R,n}$	Q	$f_{R,n}$	Q
1	36	363	22	168	6	19
2	206	730	138	455	40	73
3	496	948	379	688	112	139
4	868	821	710	603	220	220
5	—	—	—	—	364	291
6	—	—	—	—	552	300
7	—	—	—	—	765	280

<sup>a</sup> Frequency values in kHz.

**Table 2.** Resonance frequencies estimated at various modes for cantilevers of different thickness. Thickness calculated from the fundamental mode was used to estimate the higher frequency modes. From the fundamental frequency, the thickness of the 7  $\mu\text{m}$  thick cantilever was found to actually be 6.5  $\mu\text{m}$ , the 4  $\mu\text{m}$  cantilever was the same as specified by the manufacturer and the 1  $\mu\text{m}$  cantilever was found to be 1.1  $\mu\text{m}$ .

n	Mode		
	7 $\mu\text{m}$	4 $\mu\text{m}$	1 $\mu\text{m}$
	$f_{R,n}^{\text{theo}}$	$f_{R,n}^{\text{theo}}$	$f_{R,n}^{\text{theo}}$
1	36	22	6
2	224	139	39
3	627	389	109
4	1229	761	214
5	2031	1258	354
6	3034	1880	529
7	4238	2626	739

<sup>a</sup> Frequency values in kHz.

ues in a vacuum. This shift is mainly due to the additional added apparent mass (also called virtual mass) which the vibrating cantilever has to displace in the medium. This extra mass depends on the viscosity and density of the medium surrounding the cantilever. In air, the deviation is found to be about 0.5% at all modes [16, 18, 19]. However, we neglect the effect of the virtual mass of air in our present calculations. The parameter most affected is the quality factor. It decreases by almost three orders of magnitude from a vacuum to air. It is considered as one of the fitting parameters while determining the resonance frequency from the frequency response curve (equation (5)).

The resonance frequencies and the quality factors measured at various modes are shown in table 1. The corresponding frequency values estimated theoretically from equation (2) are given in table 2. The measured values deviated from estimated values. For the 7  $\mu\text{m}$  thick cantilever the deviation at mode 4 was about 30% from the theoretical value, for the 4  $\mu\text{m}$  thick cantilevers it was about 7%, while for the 1  $\mu\text{m}$  cantilevers at mode 7 it was about 1%. We believe that the deviation originates from defects in the cantilever. In the first mode, as the entire cantilever is vibrating with

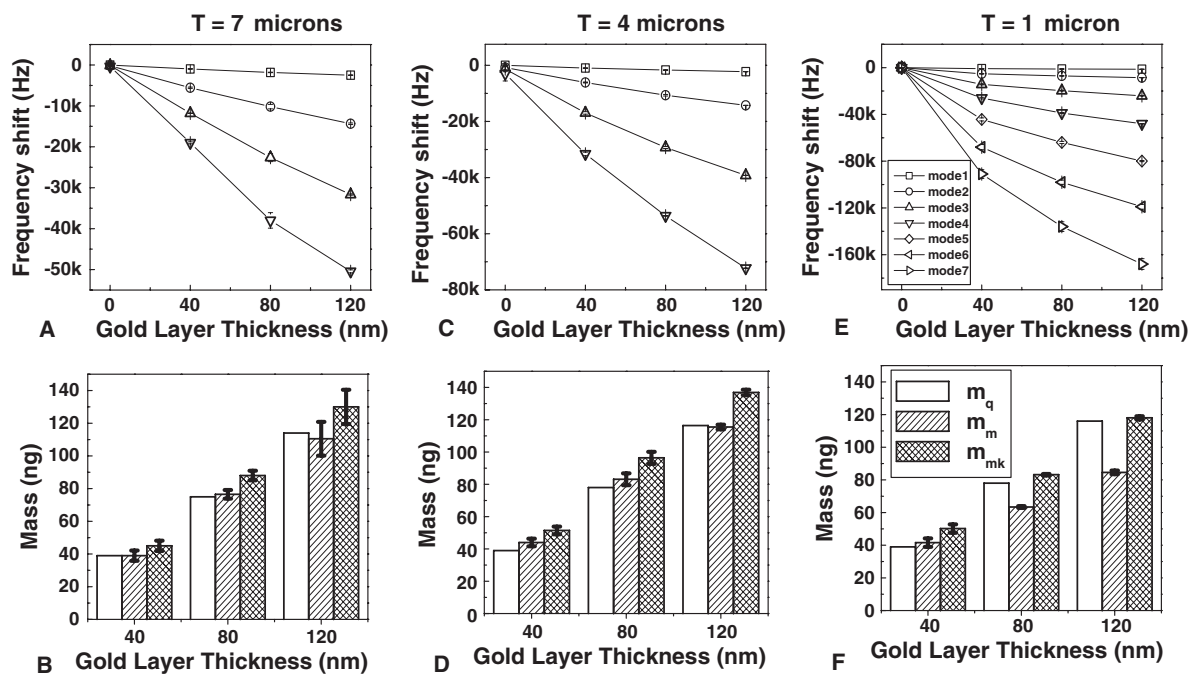


**Figure 4.** Frequency shift measured and the corresponding mass calculated at various modes. (A), (C), (E) Frequency shifts obtained for 40 nm, 80 nm and 120 nm thick gold layers deposited on 7  $\mu\text{m}$ , 4  $\mu\text{m}$  and 1  $\mu\text{m}$  thick cantilevers, respectively. (B), (D), (F) Corresponding average mass values calculated from all modes for each thickness. The three mass histogram columns for each gold layer thickness correspond to the values calculated considering dimensions (white column, equation (6)), 'mass only' change (hatched column, equation (7)) and 'mass and spring constant' change (meshed column, equation (8)), respectively. The masses calculated from the dimensions of the gold layers are 39 ng, 78 ng and 116 ng, respectively. The spring constant for the 7 and 4  $\mu\text{m}$  cantilevers did not change until 120 nm of gold, but for the 1  $\mu\text{m}$  cantilevers it changed at 80 nm of gold.

**Table 3.** The values of the calibration constant  $C$  (see equation (4)).

$n$	$C_{7\ \mu\text{m}}$	$C_{4\ \mu\text{m}}$	$C_{1\ \mu\text{m}}$
1	1	1	1
2	0.9128	0.9857	1.0060
3	0.7841	0.9637	1.0099
4	0.7009	0.9209	1.0134
5	—	—	1.0155
6	—	—	1.0304
7	—	—	1.0223

its only node near the hinge, the minor defects inside the cantilever are not contributing to the deviation. With higher modes of vibration a larger part of the cantilever participates in the movement due to the increased number of nodes. Hence the effect of internal defects will be more pronounced at the higher modes compared to the first mode. To account for such discrepancies from the measured values of higher modes of resonance we have introduced a constant  $C$  as a calibration factor as shown in equation (3). The values obtained for the calibration factor are shown in table 3. For 1  $\mu\text{m}$  they are close to 1 indicating fewer defects compared to the 7  $\mu\text{m}$  cantilever, with more defects.

#### 4.4. Frequency shift for mass loading

The difference in the resonance frequency values obtained before gold coating and after gold coating is plotted in figures 4(A), (C), (E). The graphs clearly indicate that for

each layer of gold (mass addition), the change in resonance frequency increased with the mode number.

Equations (7) and (8) were used to calculate the mass loaded on the cantilever. The values are compared to the mass calculated from the thickness measured with a quartz crystal microbalance during deposition (equation (6)). The results are plotted in a histogram as shown in figures 4(B), (D), (F). Each mass value is the average calculated from all the modes and the standard deviation is indicated as an error bar. For the 7 and 4  $\mu\text{m}$  thick cantilevers the mass measured matches quite well with the mass determined using the quartz microbalance for all thickness values of gold. While for the 1  $\mu\text{m}$  thick cantilever the effect on the spring constant can already be observed at 80 nm of gold layer thickness. The reference cantilevers without gold coating showed no frequency shift, as expected.

#### 4.5. Higher harmonics offer better sensitivity

The gold layer thickness of 40 nm (distributed load of 39 ng) has resulted in a 'mass only' effect on all cantilevers. There was no influence of spring constant until this thickness. A 3D plot of frequency shift (actual frequency shift is negative) with mode number and cantilever thickness corresponding to 40 nm of gold layer is plotted in figure 5 (unavailable values are displayed as zero). For the 1  $\mu\text{m}$  thick cantilever, the frequency shift of 91 kHz at mode 7 is two orders of magnitude larger than 834 Hz at mode 1. In terms of mass responsivity (inverse of frequency sensitivity), they measure 0.43 pg Hz<sup>-1</sup> at mode 7

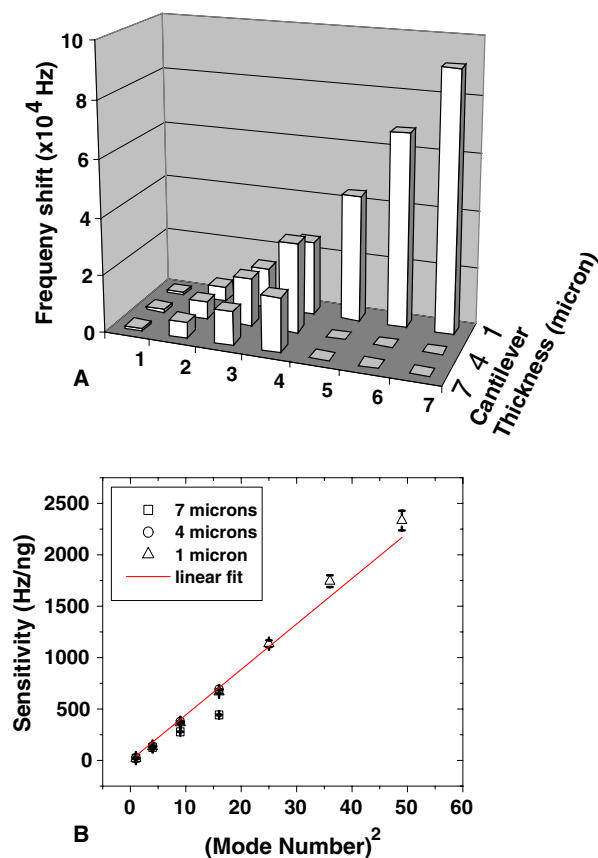


**Figure 5.** (A) The frequency shifts measured as a function of mode number and cantilever thickness corresponding to a distributed mass load of 39 ng (unavailable values are shown as zero). (B) The sensitivity is a linear function of mode number squared for every cantilever thickness.

and 47  $\text{pg Hz}^{-1}$  at mode 1. The sensitivity defined as the ratio of frequency shift to unit mass loaded is a linear function with the square of the mode number (see figure 5).

## 5. Discussion

The three important observations in our investigation are: (1) Higher modes of vibration offer a sensitivity at least two orders of magnitude higher than the fundamental mode. (2) The quality factor increases with the mode number thus helping to achieve higher sensitivity. (3) The spring constant remains unaffected for a deposited distributed gold layer thickness of at least 4% of the cantilever thickness.

A frequency shift of 0.8 kHz at mode 1 and 91 kHz at mode 7 was observed for the 1  $\mu\text{m}$  thick cantilever with a 40 nm thick gold layer (figure 5(A)). This indicates an unprecedented increase in sensitivity by two orders of magnitude at higher modes compared to lower modes for the same amount of mass load. The corresponding mass sensitivity values are 940  $\text{ag Hz}^{-1} \mu\text{m}^{-2}$  for mode 1 and 8.6  $\text{ag Hz}^{-1} \mu\text{m}^{-2}$  for mode 7. This fact shows the advantage of exploiting large frequency changes from higher modes and increasing the sensitivity of the cantilever to measure smaller masses. With a minimum detectable frequency change of 1 Hz

in our system, the best mass resolution possible is 0.43 pg at mode 7 for a 1  $\mu\text{m}$  thick cantilever.

For the same 40 nm gold layer, the sensitivity of 442  $\text{Hz ng}^{-1}$  for 7  $\mu\text{m}$ , 690  $\text{Hz ng}^{-1}$  for 4  $\mu\text{m}$  and 667  $\text{Hz ng}^{-1}$  for 1  $\mu\text{m}$  at mode 4 indicates that irrespective of cantilever thickness the frequency shift obtained is of about the same range, especially for the 4 and 1  $\mu\text{m}$  cantilevers, even though their resonance frequency values differ by 490 kHz (figure 5(B) and table 1). It leads to an important conclusion that for given length and width of the cantilever, sensitivity remains almost the same at all modes (at least up to mode 4) irrespective of cantilever thickness. The discrepancy in the sensitivity is attributed to the fact that each array was separately coated. For a given frequency span, thinner cantilevers have more modes than thicker cantilevers (figure 3). This fact enables us to access higher modes and exploit higher mass sensitivity using thinner cantilevers. Furthermore, up to a mass load for which the spring constant remains unaffected, the sensitivity behavior is linear with square of the mode number (figure 5(B)). The increase in sensitivity is also attributed to the increase in quality factor with mode number (table 1). A similar increase in quality factor and enhanced mass sensitivity at higher modes by two orders of magnitude was also observed for a point mass load on the apex of the cantilever [20]. These observations lead to an important conclusion that the mass sensitivity of cantilever sensors can be increased by working at higher modes without changing their physical parameters. Furthermore, larger physical dimensions give an added advantage of a larger surface area for accommodating more adsorbates and amplifying the mass response.

In figure 4 the mass calculated from a quartz crystal microbalance is slightly less than the mass calculated from the cantilevers. This is because the cantilever array was kept in the center directly under the evaporated gold while the quartz microbalance was placed away from center. This geometrical arrangement leads to an underestimation of the real gold thickness from the quartz microbalance and is a systematic feature which we cannot avoid. Furthermore the difference between the mass calculated using equations (7) and (8) decreases with increasing cantilever thickness, indicating that both equations result in the same mass value for thicker cantilevers where the value of the spring constant is unaffected due to additional gold layers.

Figure 4 reveals that for a gold layer thickness of at least 4% of the cantilever thickness the value of the spring constant is unaffected. Increase in the effective spring constant of the cantilever compensates for the frequency shift obtained by mass change. This fact is clear already at 80 nm gold on the 1  $\mu\text{m}$  thick cantilever. Hence, as soon as the spring constant of the cantilever starts to get affected, the linear dependence of negative frequency shift on mass ceases. The mass value calculated due to the 'mass only' effect ( $m_m$ ) is underestimated if stiffness is affected and the 'mass and spring constant' effect ( $m_{mk}$ ) is overestimated if stiffness is not affected. Results also imply that the linear range of mass detection for thin cantilevers is smaller than that of thick cantilevers (40 nm for the 1  $\mu\text{m}$  cantilever and 120 nm for the 7  $\mu\text{m}$  cantilever). However, it should be noted that the limiting factor for maximum thickness of the deposited layer before it changes the effective stiffness of the cantilever also depends on the elastic modulus of the

deposited layer. For soft biological materials like DNA, protein or cells, the elastic modulus is at least six orders of magnitude smaller than for gold [21]. Hence for a monolayer of biological molecules on the cantilever the effect of stiffness can be neglected. The frequency shift obtained involving measurements of biological samples will only be due to mass with the cantilevers investigated here.

Using cantilever arrays, statistics for a particular behavior can be obtained in a single experiment. Furthermore, by selectively functionalizing them for sensing applications, multiple target sensing at the same time is possible including the reference cantilever for better interpretation of results. In the present investigation, we have used different thicknesses of gold layers along with bare uncoated cantilevers for reference in a single cantilever array (figure 1(B)). For an array as shown in figure 2, not all the cantilevers have exactly the same resonance frequency. This indicates the dependence of resonance frequency on mechanical properties. Even though all cantilevers are microfabricated in a similar way to obtain the same dimensions, they can never be exactly the same due to process limitations. These small nuances are noted in the <0.1% deviation of the resonance frequencies in a single array. Furthermore, the absence of anomalous peaks in the resonance peak spectrum (figure 3) for the cantilevers used indicates that the spectra are devoid of any resonance frequencies from other parts of the measurement system. The amplitude distribution of the peaks is a sensitive parameter of the position of the laser beam on the cantilever. As the position of the laser beam is fixed on the cantilever apex during the entire sweep, small variations around this position result in different amplitudes of the resonance peaks. An optimized position is chosen to achieve the maximum amplitude for all modes. Also, the amplitude of vibration at higher modes is large for thinner cantilevers, making it possible to detect using optical techniques.

Theoretically estimated values of frequency at higher modes did not match with the measured values (tables 1 and 2). We attribute this to internal defects in the cantilever. These defects will affect the resonance frequencies especially at higher modes due to increase in the number of nodes and antinodes. They decrease the effective stiffness of the cantilever, decreasing the resonance frequency of vibration. This argument is supported by the observed etching artifacts in cantilevers using optical microscopes (figures not shown). These defects were more pronounced for 7 and 4  $\mu\text{m}$  thick cantilevers compared to the 1  $\mu\text{m}$  cantilever. This may be because 7 and 4  $\mu\text{m}$  cantilevers were wet etched while the 1  $\mu\text{m}$  one was dry etched. To compensate for such defects we have introduced a calibration factor as shown in equation (3). The calibration factors (table 3) indicate more defects for the 7  $\mu\text{m}$  thick cantilever.

## 6. Conclusions

Clean frequency spectra with peaks corresponding to various modes of vibration are obtained for different cantilever thicknesses. The vibrations of the fundamental and the next two modes were visualized using SEM. For a fixed length and width, thinner cantilevers exhibit more modes in a given frequency span. For uniform gold deposition on the cantilever,

the increase in mass sensitivity is linear with the square of the mode number. A sensitivity increase of two orders of magnitude is obtained from mode 1 to mode 7 with a minimum sensitivity of  $8.6 \text{ ag Hz}^{-1} \mu\text{m}^{-2}$  and mass resolution of 0.43 pg at mode 7 for the 1  $\mu\text{m}$  thick cantilever. Our results indicate that mass sensitivity using resonating nanomechanical microcantilevers can be increased by operating them at higher modes, thus keeping the larger dimensions of the cantilever and exploiting the larger surface area required for biological sensing.

## Acknowledgments

We thank Alex Bietsch and Marko Dorrestijn for fruitful discussions. Financial support is acknowledged from the Swiss National Foundation (National Center of Competence in Research), Commission for Technology and Innovation (Technology Oriented Program (TOP) NANO21), the ELTEM Regio network, G H Endress Foundation and the IBM Zurich Research Laboratory.

## References

- [1] Yang Y T, Callegari C, Feng X L, Ekinci K L and Roukes M L 2006 Zeptogram-scale nanomechanical mass sensing *Nano Lett.* **6** 583
- [2] Ekinci K L and Roukes M L 2005 Nanoelectromechanical systems *Rev. Sci. Instrum.* **76** 061101
- [3] Ilic B, Craighead H G, Krylov S, Senaratne W, Ober C and Neuzil P 2004 Attogram detection using nanoelectromechanical oscillators *J. Appl. Phys.* **95** 3694
- [4] Craighead H G 2000 Nanoelectromechanical systems *Science* **290** 1532
- [5] Calleja M, Nordstro M, Ivarez M A, Tamayo J, Lechugaa L M and Boisen A 2005 Highly sensitive polymer-based cantilever-sensors for dna detection *Ultramicroscopy* **105** 215
- [6] Chen G Y, Thundat T, Wachter E A and Warmack R J 1995 Adsorption-induced surface stress and its effects on resonance frequency of microcantilevers *J. Appl. Phys.* **77** 3816
- [7] Wachter E A and Thundat T 1995 Micromechanical sensors for chemical and physical measurements *Rev. Sci. Instrum.* **66** 3662
- [8] Pinnaduwa L A, Hawk J E, Boiadjev V, Yi D and Thundat T 2003 Use of microcantilevers for the monitoring of molecular binding to self-assembled monolayers *Langmuir* **19** 7841
- [9] Nugaeva N, Gfeller K Y, Backmann N, Lang H P, Duggelin M and Hegner M 2005 Micromechanical cantilever array sensors for selective fungal immobilization and fast growth detection *Biosens. Bioelectron.* **21** 849
- [10] Battiston F M, Ramseyer J P, Lang H P, Baller M K, Gerber Ch, Gimzewski J K, Meyer E and Güntherodt H-J 2001 A chemical sensor based on a microfabricated cantilever array with simultaneous resonance-frequency and binding readout *Sensors Actuators B* **77** 122
- [11] Gfeller K Y, Nugaeva N and Hegner M 2005 Micromechanical oscillators as rapid biosensor for the detection of active growth of *escherichia coli* *Biosens. Bioelectron.* **21** 528
- [12] Rast S, Wättinger C, Gysin U and Meyer E 2000 Dynamics of damped cantilevers *Rev. Sci. Instrum.* **71** 2772
- [13] Meyer G and Amer N M 1988 Novel optical approach to atomic force microscopy *Appl. Phys. Lett.* **53** 1045

- [14] Lang H P *et al* 1998 Novel sequential position readout from arrays of micromechanical cantilever sensors *Appl. Phys. Lett.* **72** 383
- [15] Young D and Felgar R P 1949 Tables of characteristic functions representing normal modes of vibration of a beam *The Univ. Texas Publ.* **44** 1
- [16] Chon J W M, Mulvaney P and Sader J E 2000 Experimental validation of theoretical models for the frequency response of atomic force microscope cantilever beams immersed in fluids *J. Appl. Phys.* **87** 3978
- [17] Herman D, Gaitan M and DeVoe D 2001 MEMS test structures for mechanical characterization of vlsi thin films *Proc. SEM Conf. (Portland, OR, June 2001)*
- [18] Elmer F-J and Dreier M 1997 Eigenfrequencies of a rectangular atomic force microscope cantilever in a medium *J. Appl. Phys.* **81** 7709
- [19] Maali A, Hurth C, Boisgard R, Jai C, Cohen-Bouhacina T and Aiméa J-P 2005 Hydrodynamics of oscillating atomic force microscopy cantilevers in viscous fluids *J. Appl. Phys.* **97** 074907
- [20] Dohn S, Sandberg R, Svendsen W and Boisen A 2005 Enhanced functionality of cantilever based mass sensors using higher modes *Appl. Phys. Lett.* **86** 233501
- [21] Takai E, Costa K D, Shaheen A, Hung C T and Guo X E 2005 Osteoblast elastic modulus measured by atomic force microscopy is substrate dependent *Ann. Biomed. Eng.* **33** 963